

$^{99,101}\text{Ru}$ NMR study of the Ru-site vacancies in $\text{SrRu}_{1-x}\text{O}_3$ compoundsZ. H. Han,^{1,*} J. I. Budnick,¹ W. A. Hines,¹ P. W. Klamut,^{2,3} B. Dabrowski,^{2,3} and M. Maxwell³¹*Department of Physics and Institute of Materials Science, University of Connecticut, Storrs, Connecticut 06269, USA*²*Materials Science Division, Argonne National Laboratory, Argonne, Illinois 60439, USA*³*Department of Physics, Northern Illinois University, DeKalb, Illinois 60115, USA*

(Received 21 February 2005; revised manuscript received 12 April 2005; published 30 June 2005)

It has been shown previously that the synthesis of SrRuO_3 in an oxygen environment produces nonstoichiometric $\text{SrRu}_{1-x}\text{O}_3$ compounds with randomly distributed vacancies on the Ru sites, along with a significant reduction in the ferromagnetic ordering temperature [Dabrowski *et al.*, Phys. Rev. B **70**, 014423 (2004)]. In order to gain insight into the suppression of ferromagnetism, an investigation of the short-range order, Ru magnetic moment, and Ru valence state has been carried out. Local studies utilizing $^{99,101}\text{Ru}$ zero-field, spin-echo nuclear magnetic resonance, along with complementary dc magnetization and x-ray diffraction, revealed that the Ru paramagnetic moment above the ordering temperature decreases only slightly from the Ru^{4+} low-spin ($S=1$) value as vacancies are introduced into the Ru sites. On the other hand, the ordered Ru moment measured by low-temperature hysteresis is strongly suppressed along with the ordering temperature. The results presented here do not support the idea of an increase in the average Ru valence state from 4+ to 5+ by the creation of some amount of local Ru^{5+} .

DOI: 10.1103/PhysRevB.71.214432

PACS number(s): 75.90.+w, 76.60.Lz, 81.40.Vw

I. INTRODUCTION

SrRuO_3 , with an ordering temperature of $T_c \approx 160$ K, is the only known $4d$ transition-metal oxide that is ferromagnetic. Values as high as $1.6\mu_B$ have been reported for the ordered Ru magnetic moment in the ferromagnetic state; however, the magnetization has not reached saturation in the highest fields utilized.¹ In the paramagnetic state, the Ru moment ($\approx 2.8\mu_B$) is consistent with Ru^{4+} in the low-spin configuration ($S=1$). SrRuO_3 has been described as a highly correlated, narrowband itinerant ferromagnet with a metallic-like conductivity behavior that is characterized as a “bad metal.”² Despite its robust ferromagnetism, the magnetic ordering temperature can be easily suppressed by variations in sample synthesis as well as elemental substitution (for a review, see Ref. 3). In a recent work on a series of $\text{SrRu}_{1-x}\text{O}_3$ perovskites by Dabrowski *et al.*, it was shown how the introduction of Ru-site vacancies reduced the ferromagnetic ordering temperature from 163 K to 45 K when x was increased to ≈ 0.12 .⁴ In addition, Dabrowski *et al.*⁴ describe in detail how various synthesis methods can be used to create the Ru-site vacancies and affect the sample quality. The work reported here presents results obtained from nuclear magnetic resonance (NMR), dc magnetization, and x-ray diffraction (XRD) on selected $\text{SrRu}_{1-x}\text{O}_3$ samples in order to explore the relationship between the Ru-site vacancies, Ru magnetic moment, and Ru valence state.

II. SAMPLE PREPARATION AND EXPERIMENTAL PROCEDURE

Three polycrystalline samples of nominally stoichiometric SrRuO_3 and one intentionally nonstoichiometric polycrystalline sample, nominally $\text{SrRu}_{0.92}\text{O}_3$, were synthesized from the appropriate mixtures of SrCO_3 and RuO_2 (prefired in air at 600 °C) powders using a solid-state reaction method.⁴ [In

earlier work, see Ref. 4, it was determined that two properties of RuO_2 presented serious problems during the synthesis: (1) RuO_2 is hygroscopic at ambient conditions (leading to weighing errors) and (2) RuO_2 is volatile at elevated temperatures. The problems were solved by first thoroughly drying the RuO_2 powder and then starting the calcination of the SrCO_3 and RuO_2 mixtures at low temperatures for very short times.] The mixed powders were pressed into pellets, fired in air, and reground several times. This sequence was carried out at various temperatures, starting at 800 °C and concluding at a sintering temperature of 1100 °C. These as-sintered powders were the starting materials for the four samples studied in this work. Sample one, designated “parent SrRuO_3 ,” was an as-sintered powder prepared at stoichiometry and with no further heat treatment. Sample two, designated “ambient SrRuO_3 ,” was an as-sintered powder prepared at stoichiometry and annealed twice under flowing oxygen at 1050 °C for 10 h. Sample three, designated “high-pressure SrRuO_3 ,” was an as-sintered powder prepared at stoichiometry and annealed twice under 600 atm oxygen at 1050 °C for 10 h. Sample four, designated “high-pressure $\text{SrRu}_{0.92}\text{O}_3$,” was an as-sintered powder prepared with a nonstoichiometric composition Ru/Sr ratio of 0.92 and annealed under 600 atm oxygen at 1060 °C for 10 h. The four samples, along with a summary of their magnetic properties (see below), are listed in Table I.

Conventional (XRD) analysis was carried out on the four powder samples using a Bruker diffractometer with $\text{Cu } K\alpha_1$ radiation ($\lambda = 1.5406$ Å). The patterns were recorded over the range $20^\circ \leq \theta \leq 85^\circ$ with a 2θ step of 0.02° . Within the sensitivity limit ($\approx 3\%$), all four samples were single phase with the GdFeO_3 -like orthorhombic structure. In addition, dc magnetization measurements were carried out on a Quantum Design MPMS SQUID magnetometer for temperatures $5 \text{ K} \leq T \leq 350 \text{ K}$ and magnetic fields up to 50 kOe. In this work, zero-field, spin-echo NMR spectra were obtained at 1.3 K

TABLE I. Magnetic properties of $\text{SrRu}_{1-x}\text{O}_3$ compounds.

Sample	T_c^{dc} (K)	T_c^{ac} (K) ^a	μ_z (μ_B)	H_c (Oe)	Θ (K)	μ_{eff} (μ_B)	n (f.u. ⁻¹)
Parent SrRuO_3	162 ± 1	163	1.4_0	2000	164	2.7_2	1
Ambient SrRuO_3	150 ± 3	161	1.2_5	3500	153	2.6_6	0.9_3
High-press. SrRuO_3	85 ± 2	86	0.8_6	4500	98	2.6_1	0.8_7
High-press. $\text{SrRu}_{0.92}\text{O}_3$	68 ± 5	67	0.7_6	6100	92	$2.5_4(2.5_7)$	$0.7_4(0.8_8)$

^aData from Ref. 4.

and 4.2 K over the frequency range from 40 to 105 MHz using a conventional two-pulse spectrometer with phase-sensitive detection. The NMR signals were optimized by adjusting the excitation power in a $\pi/2$ - τ - π pulse sequence. Once the NMR signals were optimized, the same excitation conditions were maintained over the entire frequency range of measurement. Usable spectra were obtained by averaging the NMR signals 500 to 2000 times at various frequency intervals across the spectrum.

III. RESULTS AND ANALYSIS

The magnetic properties for the four $\text{SrRu}_{1-x}\text{O}_3$ samples, which are summarized in Table I, include parameters from the ferromagnetic state below the ordering temperature as well as the paramagnetic state above the ordering temperature. Listed in column one are the three nominally stoichiometric SrRuO_3 samples along with the nominally nonstoichiometric $\text{SrRu}_{0.92}\text{O}_3$ sample. As shown in Fig. 1, a direct measure of the magnetic ordering temperature T_c was made

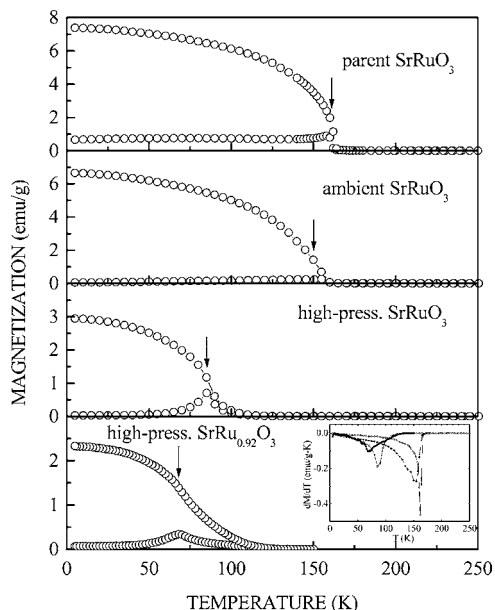


FIG. 1. Zero-field-cooled and field-cooled dc magnetization in a field of 50 Oe for the $\text{SrRu}_{1-x}\text{O}_3$ samples. The suppression of the ferromagnetic ordering temperature (indicated by arrows) is a consequence of vacancies being introduced into the Ru sites. The inset shows the derivatives of the field-cooled curves with the peak positions being T_c^{dc} . For clarity, a multiplicative factor of 2 is used except for the parent SrRuO_3 .

by observing the zero-field-cooled and field-cooled dc magnetization in a field of 50 Oe (column two, Table I). In particular, the criteria for obtaining T_c involved taking the derivative of the field-cooled magnetization versus temperature curve and defining the temperature for which the derivative is maximum (in a negative sense) as T_c^{dc} . The derivative curves for all four samples are shown as an inset in Fig. 1. It should be noted that the magnetic transition for $\text{SrRu}_{0.92}\text{O}_3$ is fairly broad, probably due to a slightly inhomogeneous distribution of Ru-site vacancies (and, therefore, a distribution in T_c) across the grains of the material.⁴ These values are consistent with results obtained previously from ac susceptibility measurements (column three).⁴ Figure 2 shows the complete hysteresis loops for the four samples which were obtained at 5.0 K. Column four lists the values for the low-temperature magnetic moment (component) per Ru atom in the ferromagnetically ordered state measured at 5.0 K and 50 kOe. These values are calculated using the nominal composition for each sample, i.e., complete occupancy of the Ru sites ($x=0$ or $n=1-x=1$) for the first three samples and $n=0.92$ for the fourth sample. Values for the coercive field, H_c , which were obtained from the hysteresis loops, are listed in column five. Columns six and seven list the parameters obtained from a Curie-Weiss fit (see Fig. 3) to the magnetic susceptibility in the paramagnetic state above the ordering temperature using

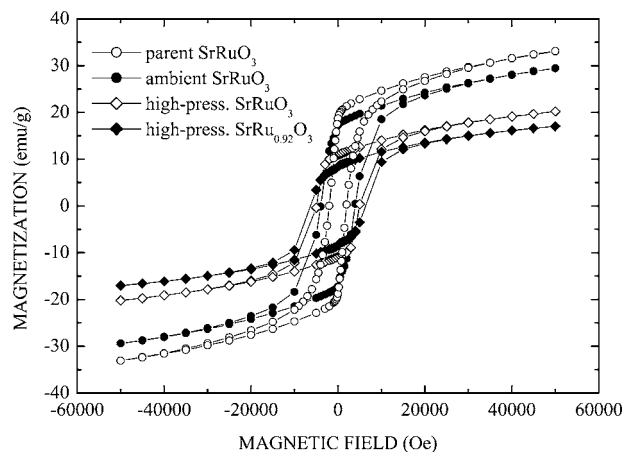


FIG. 2. Full hysteresis loops obtained at 5.0 K for the $\text{SrRu}_{1-x}\text{O}_3$ samples. As vacancies are introduced into the Ru sites, the ordered moment for Ru (obtained at 50 kOe) is greatly reduced and the coercive field is increased.

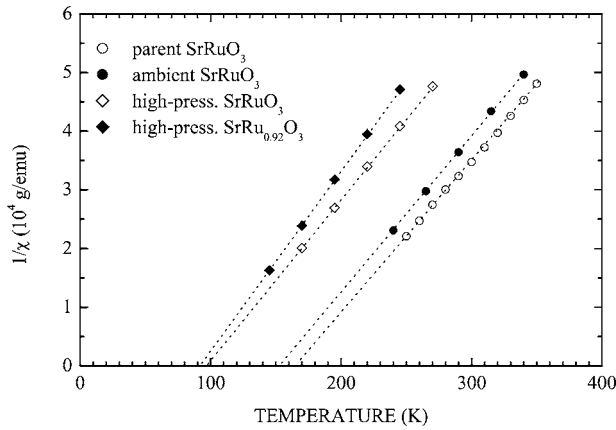


FIG. 3. Fits to the Curie-Weiss law for the SrRu_{1-x}O₃ samples. As vacancies are introduced into the Ru sites, the paramagnetic moment for Ru is only slightly reduced from a value approximately that of Ru⁴⁺ in the low-spin (*S*=1) configuration.

$$\chi(T) = \frac{n\mu_{\text{eff}}^2}{3k_B(T - \Theta)} + \chi_0, \quad (1)$$

where *n* is the concentration of Ru moments, μ_{eff} is the effective Ru moment (magnitude), k_B is the Boltzmann constant, Θ is the Curie-Weiss temperature, and χ_0 represents any temperature-independent contribution(s) such as core diamagnetism, Landau diamagnetism, and Pauli paramagnetism. Again, the nominal composition of the samples was used to calculate *n*. As discussed in detail below (Sec. IV), the four samples described in Table I are listed in order of increasing vacancy concentration at the Ru sites. The systematic suppression of the ordering temperature is accompanied by systematic behavior for the Ru moment and coercive field.

Figure 4 shows the zero-field, spin-echo NMR spectra obtained (either at 4.2 K or 1.3 K) for the four samples studied in this work. The NMR spectrum for a well-ordered SrRuO₃ phase, essentially free of impurities and defects, characterizes that obtained for the parent SrRuO₃ sample [Fig. 4(a)]. The parent SrRuO₃ spectrum consists of two sharp well-defined peaks at 64.4 MHz and 72.2 MHz corresponding to the ⁹⁹Ru and ¹⁰¹Ru isotopes, respectively, and a hyperfine field of 329 kOe.⁵ For the ⁹⁹Ru isotope, $\gamma = 0.19645$ MHz/kOe, *I*=5/2, and abundance=12.7%, while for the ¹⁰¹Ru isotope, $\gamma = 0.22018$ MHz/kOe, *I*=5/2, and abundance=17.1%. In well-ordered, single-phase SrRuO₃, the quadrupole frequencies which characterize the ⁹⁹Ru and ¹⁰¹Ru isotopes are 76 kHz and 440 kHz, respectively, reflecting the fact that the electric quadrupole moment for ¹⁰¹Ru is 5.8 times larger than that for ⁹⁹Ru.⁵ In Fig. 4, the multiplicative factors (which take into account the measurement temperature) indicate the relative NMR signal amplitudes. The NMR enhancement factor, and therefore the NMR signal amplitude, for the parent SrRuO₃ sample [Fig. 4(a)] is so large that a meaningful comparison of signal amplitude with the other three samples was not possible. Such a large enhancement factor indicates that this sample is essentially free of Ru-site vacancies which would pin the domain walls.

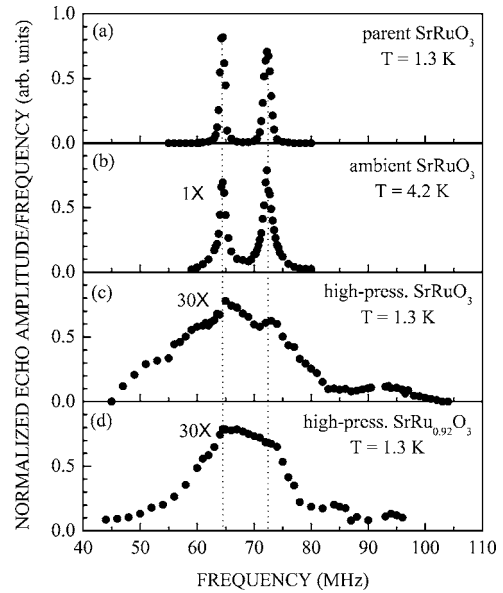


FIG. 4. Zero-field, spin-echo NMR spectra for the SrRu_{1-x}O₃ samples. The peaks at 64.4 MHz and 72.2 MHz are attributed to ⁹⁹Ru and ¹⁰¹Ru, respectively, with a hyperfine field of 329 kOe. The multiplicative factors (which take into account the measurement temperature) indicate the relative NMR signal amplitude. As vacancies are introduced into the Ru sites, an increased quadrupolar broadening results; however, there is no change in the hyperfine field. The spectra are characteristic of Ru in the Ru⁴⁺ valence state; there was no detectable NMR signal for Ru⁵⁺.

Figure 4(b) shows the NMR spectrum for the ambient SrRuO₃ sample. The two peaks, still at 64.4 MHz and 72.2 MHz, are relatively sharp and well-defined; however, a small amount of broadening is now apparent. The broadening, which is taken to be quadrupolar in origin, is a consequence of a small number of vacancies at the Ru sites. For the high-pressure SrRuO₃ sample [Fig. 4(c)], the NMR spectrum still shows the two peaks at 64.4 MHz and 72.2 MHz indicating no significant shift. However, the two peaks exhibit considerable broadening, along with structure on both the low- and high-frequency sides, indicative of a greatly enhanced quadrupole broadening due to a high concentration of vacancies at the Ru sites. Finally, the broadening for the high-pressure SrRu_{0.92}O₃ sample, which has the highest concentration of vacancies at the Ru sites, is so severe that the spectrum [Fig. 4(d)] is essentially featureless. The broad spectrum for this sample still occurs over the same frequency range (50–80 MHz) as that of the three other nominally stoichiometric SrRuO₃ samples. From the four spectra shown in Fig. 4, it can be seen that an increase in the Ru vacancy concentration (and, therefore, a decrease in the magnetic ordering temperature) results in an increase in the quadrupolar broadening; however, there is essentially no frequency shift. Since the spectra shown in Fig. 4 were obtained at a finite temperature (4.2 K or 1.3 K), the temperature dependence of the hyperfine field should be considered. It has been shown previously for SrRuO₃ that the fractional shift in frequency due to the hyperfine field temperature dependence follows the Bloch $T^{3/2}$ law, i.e.,

$$\frac{\Delta\nu}{\nu} = -B \left\{ \frac{T}{T_c} \right\}^{3/2}, \quad (2)$$

where B is a constant and T_c is the magnetic ordering temperature for the particular sample.⁵ A consideration of the ordering temperature and measurement temperature for the four samples shows that this effect is negligible and all spectra are representative of $T \approx 0$ K.

Finally, the spectra presented in Fig. 4 are characteristic of Ru atoms in the Ru^{4+} valence state where the t_{2g}^4 electrons have the low-spin ($S=1$) configuration.⁶ A careful search was made over the frequency range 100–150 MHz in order to look for the existence of the Ru^{5+} valence state where the t_{2g}^3 electrons have the high-spin ($S=3/2$) configuration.⁶ The search was carried out for both the high-pressure SrRuO_3 and $\text{SrRu}_{0.92}\text{O}_3$ samples, since these two samples have the highest concentration of vacancies at the Ru sites. For $\text{SrRu}_{0.92}\text{O}_3$, charge neutrality would require that 35% of the Ru atoms exist in the Ru^{5+} valence state. This estimate for Ru^{5+} is based on all oxygen having the O^{2-} valence state and 100% O-site occupancy.⁴ Assuming that the enhancement factor and broadening are similar for Ru^{4+} and Ru^{5+} , and allowing for the favorable factor of 2 due to the higher frequency for Ru^{5+} , the NMR signal-to-noise ratio for Ru^{5+} would be comparable to that for Ru^{4+} . A signal-to-noise ratio which is only 10% of that shown in Fig. 4(d) is well within the sensitivity of the instrumentation. No detectable NMR signal due to Ru^{5+} occurred for the two samples.

IV. DISCUSSION AND CONCLUSIONS

In an earlier work mentioned above, Dabrowski *et al.*⁴ carried out a detailed study of how various synthesis methods can be used to create vacancies at the Ru sites, used neutron powder diffraction and EDXS to determine the vacancy concentration, and established the relationship between vacancy concentration and T_c . The four samples studied in this work are identical to four samples in the earlier work. The samples listed in Table I are in order of increasing vacancy concentration at the Ru sites. The systematic suppression of the ordering temperature as measured here by dc magnetization is completely consistent with the results obtained previously by ac susceptibility.⁴ The magnetic behavior above the ordering temperature in the paramagnetic state can be described by the Curie-Weiss law yielding values for the moment (column 6) and Curie-Weiss temperature (column 7). It can be seen that the suppression of the ordering temperature T_c is accompanied by similar behavior in the Θ value obtained from the Curie-Weiss fits. The paramagnetic moment values were calculated by assuming the *nominal* concentration for Ru, i.e., 1.00 per formula unit for the first three “stoichiometric” SrRuO_3 samples and 0.92 per formula unit for the high-pressure $\text{SrRu}_{0.92}\text{O}_3$ sample. A look at the small systematic decrease in the paramagnetic moment values listed in column 6 may lead one to assume that, perhaps, this is a simple dilution effect and that the paramagnetic moment value for the remaining Ru atoms remains essentially constant as the vacancies are introduced into the Ru sites. In particular, the slightly reduced moment values ob-

tained for the ambient and high-pressure SrRuO_3 samples ($2.66\mu_B$ and $2.61\mu_B$, respectively) are a consequence of using the nominal concentration (1.00 per formula unit) instead of a concentration that is slightly smaller due to the existence of some vacancies. On the other hand, if the Ru moment is assumed to have the constant value of $2.72\mu_B$, i.e., the value obtained for the parent SrRuO_3 sample which is taken to be vacancy-free ($n=1$ per formula unit), values can then be calculated for the effective Ru moment concentration. From the Curie-Weiss law fits, $n=0.93$, 0.87 , and 0.74 were obtained for the ambient SrRuO_3 , high-pressure SrRuO_3 , and high-pressure $\text{SrRu}_{0.92}\text{O}_3$ samples, respectively (see column eight, Table I). Although the calculations are limited by the uncertainty in the moment values, they are consistent with the NMR spectra in that they reflect the increase in vacancies at the Ru sites. As concluded by Dabrowski *et al.*,⁴ the process of vacancy formation in the “stoichiometric” samples was attributed to using oxygen in the synthesis and could be strongly enhanced by using high-pressure oxygen annealing. It is apparent, however, that the assumption of a simple dilution model leads to an overestimate for the vacancy concentration, and some small reduction in the effective Ru moment value must occur. Furthermore, the nominal value of 0.92 Ru per formula unit for high-pressure $\text{SrRu}_{0.92}\text{O}_3$ was assigned from the initial Ru/Sr ratio for the powders used in the synthesis. In fact, an EDXS measurement yielded a value of 0.88 Ru per formula unit for the actual concentration.⁴ Using this value for the Ru concentration would result in a somewhat higher moment value of $2.57\mu_B$, indicating that the moment decreases by only 5.5% as Ru-site vacancy concentration x is increased up to 0.12. The paramagnetic moment value of $2.72\mu_B$ is very close to the value calculated for Ru^{4+} in the low-spin ($S=1$, $\mu_{\text{eff}}=2.82\mu_B$) configuration. Since the moment for Ru^{5+} in the high-spin ($S=3/2$) configuration is $3.87\mu_B$, the magnetic results described above argue against the creation of Ru^{5+} as vacancies are introduced into the Ru sites.

The magnetic results obtained from the hysteresis loops below the ordering temperature in the ferromagnetic state lead to a somewhat different picture for the Ru moment behavior. From the systematic behavior of the coercive field, H_c (Table I, column five), it can be seen that the introduction of vacancies at the Ru sites enhances the pinning of the domain walls. However, the values obtained (at 5.0 K and 50 kOe) for the ordered moment are strongly reduced with the introduction of vacancies at the Ru sites, which is consistent with a previous report.⁶ The reduction, which is 46% for $x=0.12$, is far greater than a simple dilution of Ru moments due to the existence of vacancies. Although saturation is not achieved at 50 kOe, the reduction in the measured ordered moment is comparable to that observed for T_c (58%).

It is noteworthy that the introduction of vacancies into the Ru sites results in severe quadrupolar broadening of the $^{99,101}\text{Ru}^{4+}$ NMR spectrum; however, there is essentially no shift in frequency. This would indicate that the hyperfine field, and therefore the local Ru moment, remains constant. Assuming a hyperfine coupling constant $\approx (-)300$ kOe/ μ_B , which is typical for $4d$ electrons and core polarization,⁷ the $^{99,101}\text{Ru}^{4+}$ hyperfine field value of 329 kOe indicates a mo-

ment value $\approx 1.1\mu_B$. Previous neutron-diffraction measurements on SrRuO₃ indicate that the Ru moments are aligned parallel with a moment value of $1.4\mu_B$.⁸ Although there is considerable uncertainty in the hyperfine coupling constant value used above, the values obtained from NMR, neutron diffraction, and dc magnetization for the Ru moment in the magnetically ordered state are in rough agreement; however, they are significantly less than that expected for $S=1$. This is likely a consequence of the itinerant nature of this system.

As mentioned above, Cu $K\alpha_1$ XRD indicated that all four samples were single phase and had the GdFeO₃-like orthorhombic structure. Furthermore, the values obtained for the lattice parameters a , b , and c were the same for all four samples within the accuracy of the measurement and consistent with those reported previously for SrRuO₃.⁹ In an attempt to observe any small subtle differences between the XRD patterns for the four samples, careful scans were made for two high-angle peaks: (1) near 67°, which consists of the (400) and (224) reflections and (2) near 77°, which consists of the (116) reflection. Within the accuracy of the measurement, there was no apparent shift of the peaks, i.e., no apparent reduction of the unit-cell volume due to the introduction of vacancies. This is consistent with the earlier work of Dabrowski *et al.*⁴ in which a detailed structural analysis was made using high-resolution backscattering data from neutron diffraction along with Rietveld refinement methods. In their

analysis, it was concluded that the Ru—O distance (or bond length) remained essentially constant while the unit-cell volume actually increased slightly with the introduction of Ru-site vacancies. The increase in the unit-cell volume is too small to be observed by the conventional XRD methods used here.

In summary, the NMR and magnetic results reported here do not support the model of a simple increase in the average oxidation state of Ru from 4+ to 5+ by the creation of some amount of local Ru⁵⁺ as vacancies are introduced into the Ru sites. Very recent Mössbauer work on a series of SrRu_{1-x}O₃ samples by DeMarco *et al.*¹⁰ yields mixed results on the valence state issue. On the one hand, the measured isomer shifts above the ordering temperature seem to indicate a change from Ru⁴⁺ to Ru⁵⁺ as x increases. However, the measured hyperfine field below the ordering temperature remains essentially constant at the characteristic Ru⁴⁺ value of 330 kOe.

ACKNOWLEDGMENTS

Work at NIU was supported by National Science Foundation Grants No. DMR-0302617 and No. DMR-0105398. At ANL, work was supported by the U.S. Department of Energy, Office of Science, Office of Basic Energy Sciences, under contract No. W-31-109-ENG-38.

*Corresponding author. Email address: zhan@phys.uconn.edu

¹G. Cao, S. McCall, M. Shepard, J. E. Crow, and R. P. Guertin, Phys. Rev. B **56**, 321 (1997).

²L. Klein, J. S. Dodge, C. H. Ahn, J. W. Reiner, L. Mieville, T. H. Geballe, M. R. Beasley, and A. Kapitulnik, J. Phys.: Condens. Matter **8**, 10111 (1996).

³Z. H. Han, J. I. Budnick, W. A. Hines, B. Dabrowski, S. Kolesnik, and T. Maxwell, J. Phys.: Condens. Matter **17**, 1193 (2005).

⁴B. Dabrowski, O. Chmaissem, P. W. Klamut, S. Kolesnik, M. Maxwell, J. Mais, Y. Ito, B. D. Armstrong, J. D. Jorgensen, and S. Short, Phys. Rev. B **70**, 014423 (2004).

⁵M. Daniel, J. I. Budnick, W. A. Hines, Y. D. Zhang, W. G. Clark, and A. R. Moodenbaugh, J. Phys.: Condens. Matter **12**, 3857

(2000).

⁶B. Dabrowski, M. Avdeev, O. Chmaissem, S. Kolesnik, P. W. Klamut, M. Maxwell, and J. D. Jorgensen, Phys. Rev. B **71**, 104411 (2005).

⁷K. Kumagai, S. Takada, and Y. Furukawa, Phys. Rev. B **63**, 180509(R) (2001).

⁸J. M. Longo, P. M. Raccach, and J. B. Goodenough, J. Appl. Phys. **39**, 1327 (1968).

⁹H. Kobayashi, M. Nagata, R. Kanno, and Y. Kawamoto, Mater. Res. Bull. **29**, 1271 (1994).

¹⁰M. DeMarco, D. Coffey, P. Klamut, B. Dabrowski, R. Heary, M. Maxwell, S. Toorongian, and M. Haka, Phys. Rev. B **71**, 104403 (2005).